



Review

# Optimising the Use of Ultrasound in Gout: A Review from the Ground Up

Emilio Filippucci <sup>1,\*</sup> , Edoardo Cipolletta <sup>1,\*</sup> , Silvia Sirotti <sup>2</sup> and Georgios Filippou <sup>2,3</sup>

<sup>1</sup> Rheumatology Unit, Department of Clinical and Molecular Sciences, Polytechnic University of Marche, 60126 Ancona, Italy; emilio\_filippucci@yahoo.it

<sup>2</sup> Rheumatology Department, Istituto di Ricovero e Cura a Carattere Scientifico (IRCCS) Galeazzi—Sant’Ambrogio Hospital, 20157 Milan, Italy; silvia.sirotti@gmail.com (S.S.); gf.filippou@gmail.com (G.F.)

<sup>3</sup> Department of Biomedical and Clinical Sciences, University of Milan (UNIMI), 20122 Milan, Italy

\* Correspondence: edoardocipolletta@gmail.com

**Abstract:** The use of ultrasonography (US) has considerable potential for the diagnosis and monitoring of gout due to its capacity to detect monosodium urate deposits. In the last decade, a critical amount of scientific data has become available. Consensus-based definitions for ultrasonographic elementary lesions in gout have been developed, tested, and validated, as well as a semiquantitative scoring system for their quantification. Many scanning protocols have been proposed in different clinical scenarios. In this review, we formulate a set of practical suggestions for the use of the US in daily practice. We discuss the current knowledge to indicate which joints and structures are to be scanned and which elementary findings are to be evaluated according to the clinical scenario. While for some clinical settings, a quite definite scanning protocol can be indicated, others still need to be further investigated, and how to obtain the best out of the US is still entrusted to the individual experience.

**Keywords:** ultrasound; ultrasonography; crystal arthritis; monosodium urate; gout; flare; arthritis



**Citation:** Filippucci, E.; Cipolletta, E.; Sirotti, S.; Filippou, G. Optimising the Use of Ultrasound in Gout: A Review from the Ground Up. *Gout Urate Cryst. Depos. Dis.* **2024**, *2*, 86–100. <https://doi.org/10.3390/gucdd2020009>

Academic Editor: Rebecca Grainger

Received: 30 December 2023

Revised: 15 March 2024

Accepted: 26 March 2024

Published: 4 April 2024



**Copyright:** © 2024 by the authors. Licensee MDPI, Basel, Switzerland. This article is an open access article distributed under the terms and conditions of the Creative Commons Attribution (CC BY) license (<https://creativecommons.org/licenses/by/4.0/>).

## 1. Introduction

Gout is a crystal arthropathy characterised by the deposition of monosodium urate (MSU) crystals in articular and periarticular tissues [1]. It is the most common inflammatory arthritis in Western countries [2], with an estimated prevalence in American adults of 3–4% [3].

Long-standing untreated gout can lead to tophaceous deposits, chronic joint damage, renal stones, chronic kidney disease, and a variety of cardio-metabolic comorbidities [4–6].

The identification of MSU crystals by microscopic analysis is the gold standard for the diagnosis of gout [7,8]. However, the identification of MSU crystals can be challenging because joint aspiration and synovial fluid analysis require skills and facilities that are not always available, especially in primary care, where most of the patients with gout are managed. Thus, imaging techniques play an important role in the diagnosis of gout, especially in patients with atypical clinical features and uncertain diagnoses [8].

Several imaging modalities have been used to detect MSU crystal deposits, estimate their extent, and monitor changes induced by urate-lowering therapy [9]. In particular, ultrasound (US) and dual-energy computed tomography (DECT) have been shown to be accurate and reliable in the identification of MSU crystal deposits. Indeed, the US and DECT have been included in the American College of Rheumatology (ACR)/European League Against Rheumatism (EULAR) 2015 classification criteria for gout. Their important role has been confirmed in the 2018 updated EULAR evidence-based recommendations for the diagnosis of gout [7,8]. The diagnostic value of the US has been reported in a large, international, multicentric study showing that US has a high specificity for diagnosing gout [10].

The main advantages of the US include the low running costs, the widespread availability, the absence of radiation exposure, the possibility to carry out a repeatable multi-site and multi-tissue evaluation, the capability of real-time assessment, and the ability to investigate not only MSU deposits but also structural damage and inflammatory changes [8,11–13]. Moreover, the US has shown moderate to excellent reliability in several studies [14–18].

The purpose of this narrative review is to describe the optimal scanning technique and the machine settings to obtain the most out of US scans in clinical practice, with the explicit objective of maximising the diagnostic potential of US in the clinical management of gout. The manuscript aims to serve as a comprehensive guide, equipping clinicians with the knowledge required to perform US in the nuanced landscape of gout diagnosis and management.

## 2. Machine Setting Optimisation for Crystal Visualisation

The spectrum of US findings indicating crystal deposits is broad and heterogeneous. This variability depends on the size, shape, echotexture, and distribution of crystal deposits.

Compared to calcium pyrophosphate (CPP) crystals, MSU deposits may have variable echogenicity (from hypoechoic to hyperechoic) and are frequently inhomogeneous [11, 16,18,19]. They may generate posterior acoustic shadowing [16,18,20]. This aspect may contribute to differentiating MSU deposits from other hyperechoic structures and CPP crystal deposits.

When MSU deposits have a hyperechogenic appearance (similar to the bony surface), it is poorly influenced by changing the angle of insonation and reducing the gain level. In fact, hyperechoic MSU deposits remain identifiable, as well as the bone, even with a low level of gain, while other hyperechoic abnormalities such as proteinaceous debris, synovial proliferation, and other soft-tissue interfaces may become undistinguishable [11,21].

In addition, anisotropy artefacts may be a valuable resource when dealing with gout. MSU deposits are not affected by such artefacts, and they maintain their high reflectivity while the surrounding structure reduces their echogenicity. Thus, the identification of MSU deposits is easier when they are situated within tissues prone to anisotropy artefacts, such as tendons and ligaments [11,21]. On the other hand, incorrect machine settings (e.g., an excess of electronic steering of US beams or the use of the compound image) may lead to overestimation of normal hyperechoic structures such as the chondro-synovial interface.

When performing US examinations for the detection of MSU deposits, specific scanning manoeuvres and machine settings can significantly impact the quality and accuracy of the imaging. General considerations are summarised in Table 1.

**Table 1.** Tips and tricks for US imaging in gout.

Image Acquisition	
1.	Use a generous amount of gel to avoid tissue compression and to enhance the reflectivity of acoustic interfaces and the distinction between different tissues.
2.	Perform a clinically driven and tissue-oriented US examination, including common targets for MSU deposition such as the metatarsophalangeal joints, the knees, and other joints clinically relevant in the patient's history. It is important to pay more attention to hyaline cartilages and extra-articular abnormalities than in a standard US assessment of patients with rheumatoid arthritis since MSU deposits may be localised both intra- and extra-articularly. Remember the differences in the topography of crystal deposits between calcium pyrophosphate deposition (mainly within the hyaline cartilage and fibrocartilage) and MSU deposits (both intra- and extra-articular and on the outer margin of the hyaline cartilage).
3.	Carry out a multiplanar and comprehensive US evaluation of the whole anatomical area. MSU crystals may be everywhere!
4.	Assess greyscale images both in static and dynamic scans and scan suspect crystal deposits both orthogonally and obliquely to test their dependence on the angle of insonation. Perform a dynamic assessment of the double contour sign to evaluate its dynamic behaviour in order to distinguish between calcium pyrophosphate deposits and MSU deposits.
5.	Complete the US evaluation using the Doppler mode and comparative examination with the contralateral side and normal tissues.

**Table 1.** *Cont.*

US machine settings	
6.	Frequency. Choose a high-frequency transducer for joint and soft tissue imaging. The selection of a higher frequency (the higher, the better for assessing superficial tissues) is crucial as it improves spatial resolution, allowing for the detailed visualisation of small structures like MSU crystals. However, be mindful of the trade-off with tissue penetration; high frequencies limit the depth of US imaging.
7.	Gain (master gain and time gain compensation). Adjust the overall gain carefully to achieve optimal visualisation of normal tissues. Frequent adjustments may be necessary during the examination to maintain an optimal balance. Fine-tune the gain settings to optimise the contrast between different tissues and improve the distinction between normal tissues and MSU deposits. An iterative approach, comparing echoes from adjacent healthy tissue, helps in setting appropriate gain levels. Test the echogenicity of hyperechoic findings, reducing the gain level.
8.	Depth. Set the depth appropriately to encompass the region of interest. Gout-related MSU deposits are often found in superficial joints and soft tissues. Adjust the depth settings to focus on the specific anatomical area under examination.
9.	Dynamic range. Adjust the dynamic range to optimise the contrast between different tissues and improve crystal identification. The dynamic range setting affects the display of grayscale levels, enhancing the visualisation of subtle differences in tissue echoes. Proper adjustment is critical to identify MSU crystals against the background of surrounding tissues.

Specific adjustments may be needed based on the US system, patient characteristics, and the anatomical region being examined.

### 3. US Definitions for Crystal Identification in Tissues

The Outcome Measures in Rheumatology (OMERACT) US Working Group Gout Subtask Force developed and tested the reliability of consensus-based definitions for the US findings in gout [16,18].

With an agreement of >80%, consensus-based definitions were obtained for four elementary lesions: double contour (DC), tophi, aggregates, and bone erosions.

The adoption of the OMERACT definition for US imaging is of paramount importance in ensuring methodological consistency and international standardisation. Embracing the OMERACT criteria establishes a common framework, fostering uniformity in US assessments across studies, researchers, and centres. This standardised approach not only enhances the reliability and validity of research outcomes but also facilitates comparisons between studies. By promoting a shared methodology, the OMERACT definitions have contributed to the robustness of evidence-based practices in US imaging, thereby reinforcing the clinical applicability of US findings within gout research.

#### 3.1. Double Contour Sign

OMERACT definition: Abnormal hyperechoic band over the superficial margin of the articular hyaline cartilage, independent of the angle of insonation, which may be either irregular or regular, continuous or intermittent, and can be distinguished from the cartilage interface sign [16,18] (Figures 1 and 2).

The DC sign has a high specificity for the diagnosis of gout (89.0%), but its sensitivity is moderate (65.1%) [22]. However, some studies have questioned its specificity for gout, as the DC sign has been described in patients with calcium pyrophosphate deposition (CPPD), with a prevalence of 7–20% [10,23,24].

The diagnostic accuracy of the DC sign depends on joint shape and size. The shape determines the width of the acoustic window to detect the DC sign, and the knee represents the joint with the larger extent of the cartilage surface explorable by the US. The size was investigated by Löffler et al., who reported the highest sensitivity (78.8%) in medium-size joints, such as the ankle and wrist, and the best specificity in large-size joints (85.1%), such as the knee and shoulder [25].

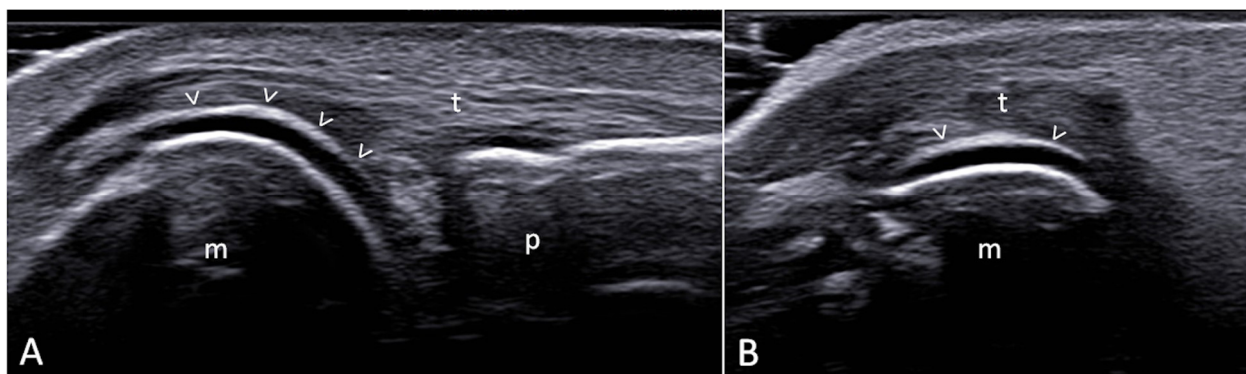


**Figure 1.** Double-contour sign (arrowheads). Hand, fifth finger, metacarpophalangeal joint. Dorsal longitudinal (A) and transverse (B) views. m = metacarpal head; p = proximal phalanx; t = finger extensor tendon. Images were acquired using a 6–18 MHz linear probe.

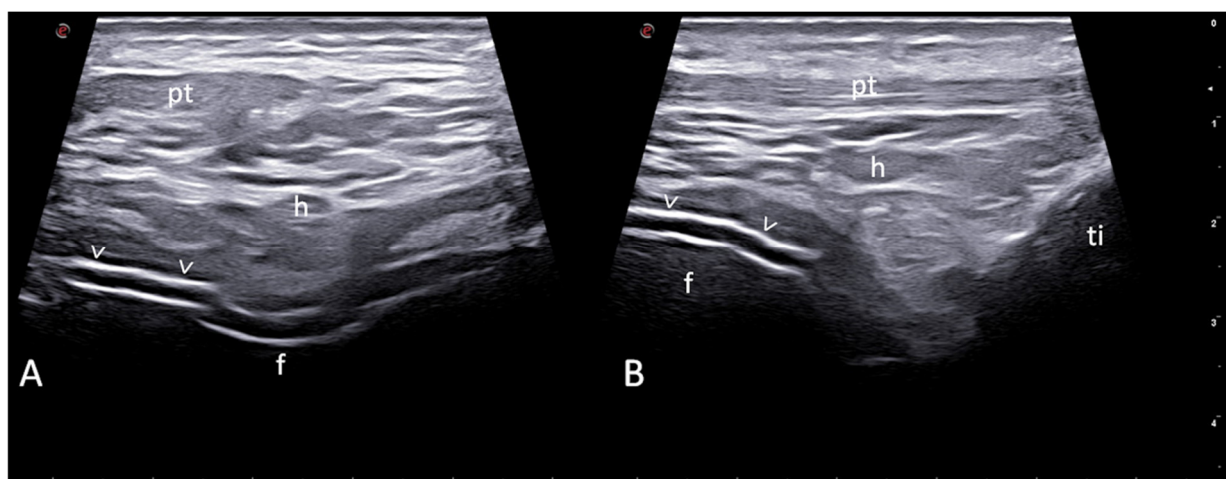


**Figure 2.** Double-contour sign (arrowheads). Knee, trochlear hyaline cartilage of the femur. Anterior transverse (A) and longitudinal (B) views. f = femoral trochlea; ti = tibia; pt = patellar tendon; h = Hoffa's fat pad. Images were acquired using a 3–11 MHz linear probe.

Particular attention should be given to avoid misinterpretations. The DC sign entails an enhancement of the chondro-synovial margin, which results in thicker than normal and is not dependent on perpendicular insonation to be visualised [16,18,26]. Another aspect to take into account is to avoid overestimation of the normal chondro-synovial interface in the presence of overlying fluid collections. For instance, the presence of even a small amount of synovial fluid can enhance the visualisation of the superficial margin of the articular cartilage. The dislocation of this fluid with the probe can help in the interpretation of this finding [21]. Finally, a dynamic assessment of the hyaline cartilage should always be performed during slow flexion and extension movements of the joint because the DC sign moves together with the subchondral bone while other hyperechoic interfaces (i.e., capsules and/or ligaments) and the pseudoDC sign of CPPD move in the opposite direction [19,27].

### 3.2. Tophi

OMERACT definition: A circumscribed, inhomogeneous, hyperechoic, and/or hypoechoic aggregation (which may or may not generate posterior acoustic shadow) may be surrounded by a small anechoic rim that may be either intraarticular or intratendinous [16,18] (Figures 3–5).

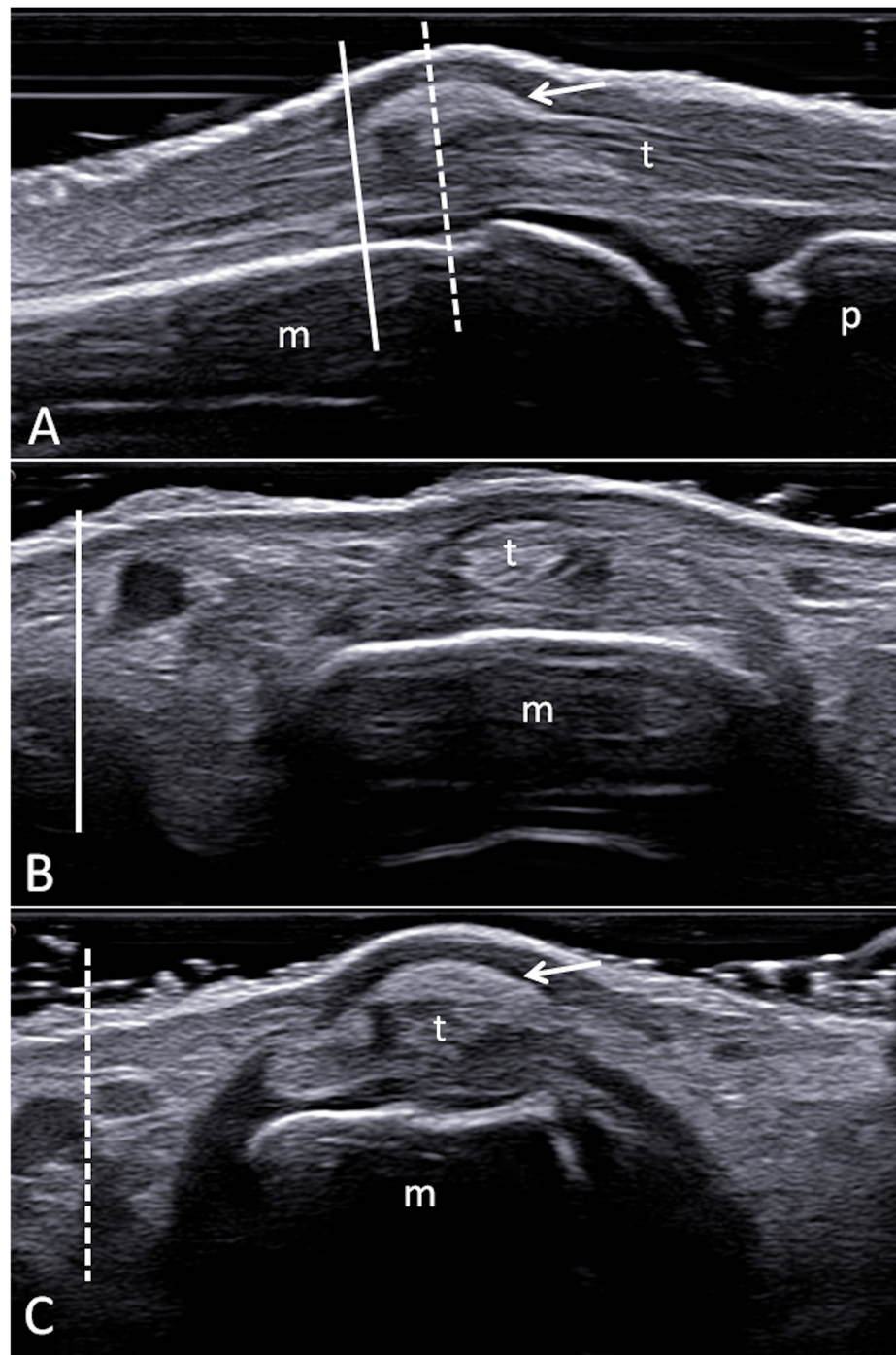


**Figure 3.** Tophaceous deposit (arrows). Hand, third finger, metacarpophalangeal joint. Dorsal longitudinal (A) and transverse (B,C) views. Transverse views (B,C) were acquired at the level of the solid (B) and dashed (C) lines, respectively m = metacarpal bone; p = proximal phalanx; t = finger extensor tendon. Images were acquired using a 6–18 MHz linear probe.

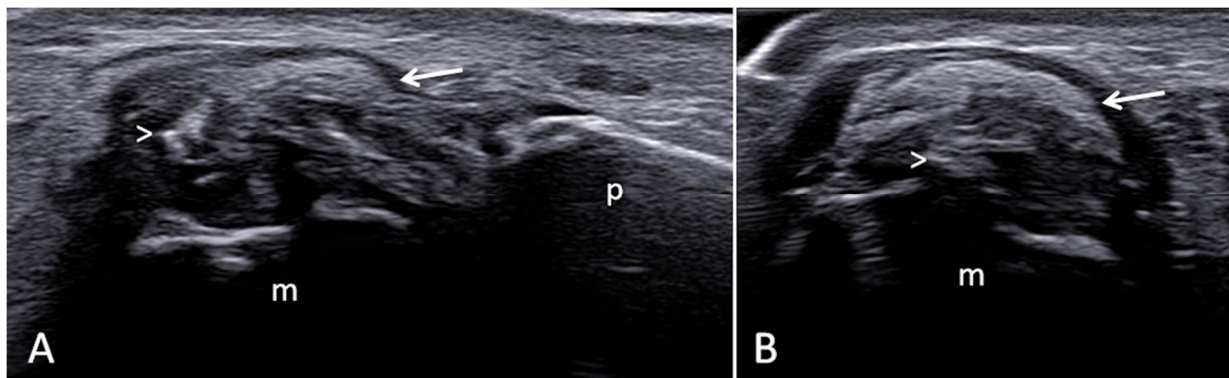


**Figure 4.** Tophaceous deposit (arrows and arrowhead). Hand, second finger, metacarpophalangeal joint. Radial aspect longitudinal (A) and transverse (B) views. m = metacarpal head; p = proximal phalanx. Note the heterogeneous texture of the tophus, which is made up of different areas with variable degrees of echogenicity. A part of the tophus generates an acoustic shadow and a pseudo interruption of the underlying bone profile. Images were acquired using a 6–18 MHz linear probe.

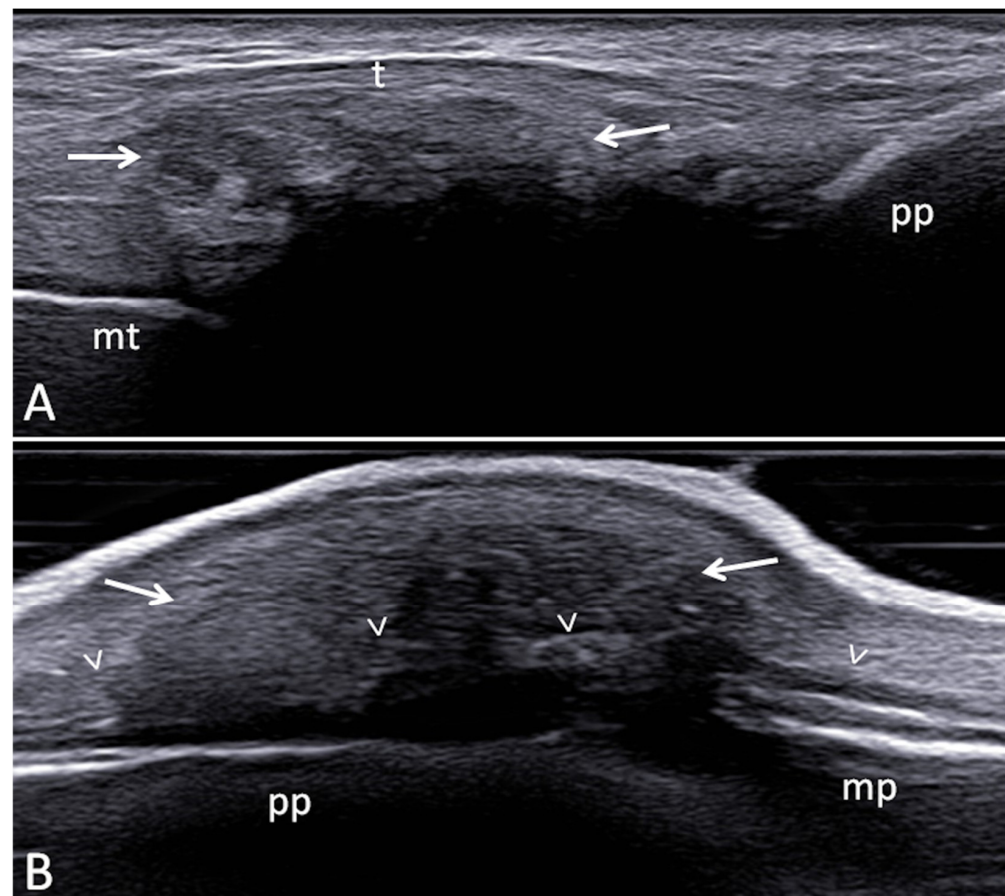


**Figure 5.** Tophaceous deposits (arrows). (A) Foot, second digit, metatarsophalangeal joint. Dorsal longitudinal view. (B) Hand, third finger, proximal interphalangeal joint. Dorsal longitudinal view. Both images show representative examples of hard tophi with complete and partial impairment of the ultrasound beam penetration and, consequently, of the underlying bony cortex visualisation. While in A, the tophus is intra-articular with a clear visualisation of the overlying extensor tendon of the finger, in B, the tophus is periarticular and englobes the finger extensor tendon that is barely detectable inside the tophaceous texture (arrowheads). mt = metatarsal bone; pp = proximal phalanx; mp = middle phalanx. Images were acquired using a 6–18 MHz linear probe.

While tophaceous deposits are a key feature in gout, their US detection was not included in the 2015 gout ACR/EULAR classification criteria. Tophi are almost exclusively found in gout, and US identification of tophi yielded a very high specificity (93.2%) but a lower sensitivity (54.3%) than the DC sign [22].

Tophi may generate a wide spectrum of US features not only in different patients but also in the same subject. Such heterogeneity depends on several factors: the size of MSU deposits (from small deposits not detectable on physical examination to clinically evident subcutaneous deposits), their outline (well or poorly defined margins), their echostructure (homogeneous or inhomogeneous deposits), and their anatomical site.

### 3.3. Aggregates

OMERACT definition: Bright hyperechoic, isolated spots too small to fulfil the tophus definition and characterised by maintaining their high degree of reflectivity when the insonation angle is changed, which may be either intraarticular or intratendinous. The aggregates can only be scored in a patient if other US features suggestive of gout, such as DC and/or tophus, are present/have previously been present at the patient level and if the aggregates are not located inside a tophus [16,18] (Figure 6).

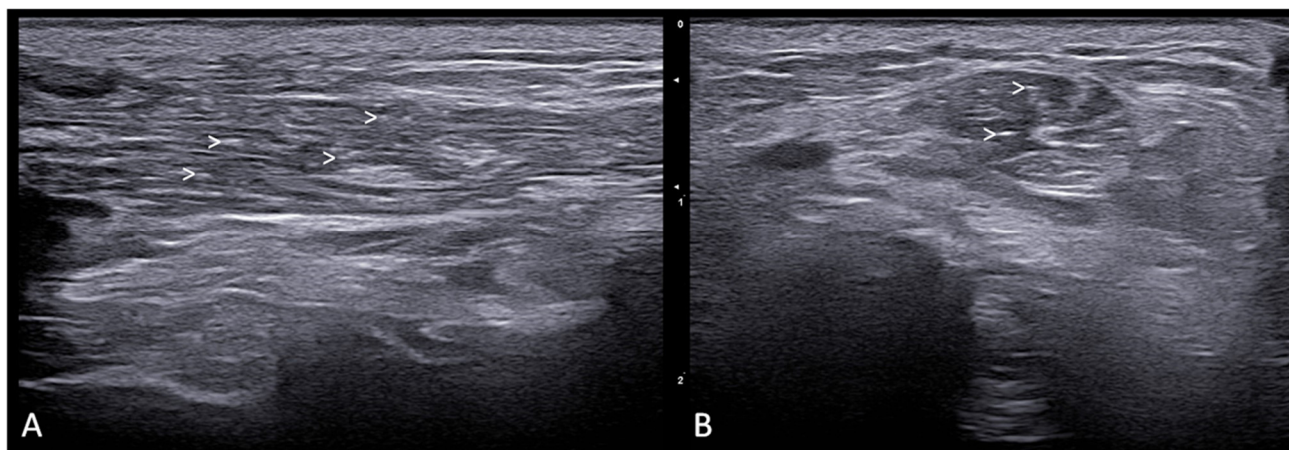


**Figure 6.** Aggregates within the tibialis anterior tendon. Ankle, tibialis anterior tendon. Anterior longitudinal (A) and transverse (B) views. Note the important derangement of the tendon fibrillar echotexture due to urate deposits appearing as iperechoic spots and dots (arrowheads). Images were acquired using a 6–18 MHz linear probe.

Aggregates are thought to be MSU deposits that are not large enough to be defined as tophi [16,18]. They may be the earliest sign of MSU deposition. However, due to an unsatisfactory specificity (32%) [28], the OMERACT US Working Group changed their definition in 2021. Indeed, intra-articular air bubbles, steroid crystals after local treatments, and other small crystal deposits may mimic small aggregates [21]. Although this definition will surely increase their specificity, it takes away their value in the early diagnosis of gout and downgrades the role of aggregates to monitoring only.

### 3.4. Bone Erosions

OMERACT definition: An intra- and/or extra-articular discontinuity of the bone surface (visible in two perpendicular planes) [16].

Although bone erosions are regarded as gout-specific US findings [16], they could also be detected in other inflammatory or degenerative arthropathies. In gout, the erosions are often multifocal, predominantly located on the medial side of the metatarsal head of the first toe, and rarely show the Doppler signal inside [29]. The US identification of bone erosions yielded a very high specificity (93.3%) and a moderate sensitivity (51.6%) for gout [22]. In fact, the typical distribution (e.g., the metatarsophalangeal joint of the first

digit) and the US appearance (usually deeper, more destructive, and filled with hyperechoic MSU deposits) make bone erosions characteristic of gout [11,21]. In addition, the presence of bone erosions at the MTP1 joint level was associated with higher scores of US-detected DC signs, tophi, and aggregates [30].

However, systematic and comparative studies should further define the specificity of US-detected bone erosions (including their shape, appearance, and size) in the classical ‘target’ joints of gout using other rheumatic diseases as controls [31,32].

#### 4. OMERACT Semiquantitative Scoring System

In 2021, the OMERACT US working group developed and tested a scoring system for MSU crystal deposits (i.e., aggregates, DC signs, and tophi). The score ranges from 0 to 3: grade 0 equals “absence” of MSU deposits, grade 1 to “possible” presence of MSU deposits, grade 2 to “definite but minimal” MSU deposition, and grade 3 to “definite and severe” MSU deposition [18].

The reliabilities of the scoring system were good for all lesions, with slightly higher intra-reader ( $\kappa$ -values 0.74–0.80) than inter-reader reliabilities ( $\kappa$ -values 0.61–0.67) in a patient-based reliability exercise. Moreover, this scoring system has been shown to be sensitive to change after a treat-to-target approach with urate-lowering therapies in independent cohorts [30,33].

#### 5. Main Applications of Ultrasound in Gout

In 2019, the Gout, Hyperuricemia and Crystal-Associated Disease Network (G-CAN) proposed a set of disease states in patients with gout: preclinical states (asymptomatic hyperuricemia, asymptomatic MSU crystal deposition, asymptomatic hyperuricemia with MSU crystal deposition), clinical states (gout, tophaceous gout, erosive gout), and gout flares (first gout flare and recurrent gout flare) [34]. Table 2 reports the main potential applications of the US in gout according to published literature and our clinical practice.

**Table 2.** Main potential applications of US in gout.

Disease State as Proposed by the G-CAN [34]	Clinical Question for US
Preclinical states	To provide evidence of MSU crystal deposition in asymptomatic hyperuricemia
Clinical states	To establish a diagnosis of gout during inter-critical phases by the visualisation of MSU deposits and by guiding the aspiration of synovial fluid
	To evaluate the burden of MSU crystal deposits, subclinical inflammation, and structural damage
	To monitor the efficacy of treatments on crystal deposition, structural damage, and subclinical inflammation
Gout flares	To diagnose gout during the first or recurrent gout flare
	To recognise painful musculoskeletal conditions not related to gout
	To treat gout flares by guiding local injections

MSU: monosodium urate; US: ultrasound.

The US scanning protocol should be tailored using data from current and previous clinical and imaging pathological findings. Moreover, the US assessment should also include the most frequently involved targets, even when asymptomatic [35,36].

Table 3 summarises the most commonly used scanning protocols in gout.

**Table 3.** Main sonographic scanning protocols used in patients with gout.

Authors	Anatomical Areas Evaluated	Bilateral Assessment	US Findings	OMERACT Definitions	RS	SE	SP	PPV	NPV
Diagnostic purposes in intercritical gout									
Peiteado et al. [14]	two joints: MTP1 joint (dorsal, medial, and plantar aspects) and knee (medial and lateral recesses and hyaline cartilage of the trochlea)	Y	Hyperechoic cloudy areas DC sign	N	SFA	97%	NR	NR	NR
Naredo et al. [15]	one joint: radiocarpal joint two tendons: patellar tendon and triceps tendon three articular cartilages: I metatarsal head dorsal and plantar cartilage, talar cartilage, and either second metacarpal cartilage (dorsal aspect) or femoral condyle cartilage	Y	Tophi DC sign Hyperechoic linear bands	N	SFA	84.6%	83.3%	91.7%	71.4%
	four joints: radiocarpal joint, midcarpal joint, MTP1 joint and knee two tendons: patellar tendon and triceps tendon three articular cartilages: I metatarsal head dorsal and plantar cartilage, talar cartilage, and either second metacarpal cartilage (dorsal aspect) or femoral condyle cartilage	Y				94.5%	71.4%	87.8%	85.7%
	two tendons: patellar tendon and triceps tendon	Y				46.2%	97.6%	97.7%	45.6%
Norkuviene et al. [37]	two joints: MTP1 joint and ankle	Y	Tophi DC sign	N	SFA	84.0%	81.0%	NR	NR
Diagnostic purposes in acute mono/oligoarthritis									
Lamers-Karnebeek et al. [38]	three joints: the most inflamed joint, MTP1 joint and knee (when the most inflamed joint was MTP1) or knee the ankle should be included)	Y	Tophi DC sign Snowstorm sign	N	SFA	96%	68%	74%	95%
Zufferey et al. [39]	one joint: the symptomatic one	N	Tophi, DC sign Aggregates	Y	SFA	60%	92%	92%	62%
	four joints: symptomatic one + knee, ankle and the MTP1 joint	Y		Y	SFA	84%	78%	82%	77%
Pattamapaspong et al. [40]	one joint: the symptomatic one	N	Tophi, DC sign Aggregates	Y	SFA	75%	89%	91%	71%
Christiansen et al. [28]	six joints: MTP1–5 joints (for tophi and DC) and knee (for DC) two tendons: peroneus tendons	Y	Tophi, DC sign	Y	SFA	93%	/	/	/
Cipolletta et al. [36]	Five joints: knees, MTP1 joints (for tophi and DC), plus the symptomatic joint One tendon: patellar tendon	Y	Tophi, DC sign	Y	SFA	91%	91%	71%	98%
Monitoring treatment efficacy and prognostic purposes									
Christiansen et al. [41]	Three joints: MTP1 joint (for tophi and DC), MTP2 joint, and knee (for DC) Two tendons: peroneal tendons and distal portion of patellar tendon (for tophi)	Y	Tophi, DC sign	Y	SFA	/	/	/	/
Peiteado [42] and Ebstein [43]	Two joints: MTP1 joint and knee (for tophi and DC)	Y	Tophi, DC sign	Y	SFA	/	/	/	/

Legend. DC: double contour, MTP1: 1st metatarsophalangeal, MTP2: 2nd metatarsophalangeal, N: no, NPV: negative predictive value, PPV: positive predictive value, RS: reference standard, SE: sensitivity, SFA: synovial fluid analysis, SP: specificity, US: ultrasound, Y: yes.

## 6. Sonographic Diagnosis of Gout in the Inter-Critical Phases in Patients with Uncertain Diagnosis

In the last decade, several US scanning protocols have been described. In 2012, Peiteado et al. [14] demonstrated the usefulness of a short US scanning protocol in the diagnosis of gout. The authors reported excellent sensitivity (97%) and feasibility (6 min) of a scanning protocol including four joints (knees and MTP1 joints) and two elementary findings (hyperechoic cloudy areas and DC sign). The main limitations of this study were the absence of a control group that did not allow for assessing the specificity of such a scanning protocol, the low number of patients, and the lack of standardised definitions for US findings. Moreover, the upper limb's structures and Achilles tendons were not evaluated, despite their involvement, which is not rare in gout.

To overcome such limits, in 2014, Naredo et al. [15] carried out a systematic multiplanar US examination of 26 joints (42 synovial recesses), 6 bursae, 8 tendons, and 20 tendon compartments, 4 ligaments, and 18 articular cartilages (30 cartilage areas) in 91 gouty patients and 42 age-matched controls. Then, a reduced scanning protocol was developed. The assessment of one joint (radiocarpal joint) for aggregates, two tendons (patellar tendon and triceps tendon) for aggregates, and three hyaline cartilages (metatarsal head's cartilage of the MTP1 joint on the dorsal and plantar scans, talar cartilage, and either metacarpal head's cartilage of the MCP2 joint on the dorsal scan or femoral condyles' cartilage on the anterior scan) for DC sign showed the best balance between sensitivity (84.6%) and specificity (83.3%), with a positive and negative predictive value of 92.0% and 71.0%, respectively. In addition, the inclusion of three more joints (midcarpal joint, MTP1 joint, and knee) for aggregates led to a very high sensitivity (94.5%) for the diagnosis of gout.

The diagnostic accuracy of the scanning protocols proposed by Peiteado et al. and Naredo et al. was compared by Bhadu et al. [44], reporting the same sensitivity, specificity, and positive and negative predictive values using both the 4-site and the 12-site examination (87.2%, 84.0%, 83.7%, and 85.6%, respectively).

In 2021, Christiansen et al. [28] suggested the use of a reduced set of anatomic sites to be scanned for diagnosing gout using OMERACT definitions for MSU deposits. In addition to MTP1 joints (for tophi and DC sign) and knees (for DC sign), the authors included MTP2–5 joints (for tophi and DC sign) and peroneal tendons (for tophi). Although it showed excellent sensitivity (93%), its specificity was not provided.

It is well known that disease duration is an important factor in determining the sensitivity of the US [10,45]. In fact, sensitivity was higher in patients with long-standing disease ( $\geq 2$  years of symptoms or with subcutaneous tophi) than in those with early disease or without subcutaneous tophi, both considering DC sign (63.4% vs. 50.9%,  $p = 0.02$ ) and tophi (50.5% vs. 33.6%,  $p < 0.01$ ) [10]. Thus, Norkuviene et al. [37] carried out a study aiming at identifying the optimal scanning protocol for the diagnosis of early gout ( $\leq 2$ -year symptom duration). A total of 36 joints (both wrists, MCP joints, proximal interphalangeal joints, knees, ankles, and MTP joints) and 2 tendons (triceps and patellar tendons) were assessed for DC sign and tophi in 60 gouty patients and 36 normouricemic subjects. The presence of tophi in the MTP1 joint and of the DC sign in the ankle yielded a sensitivity and specificity of 84% and 81%, respectively.

Although the US has shown good diagnostic accuracy in evaluating either 4 or 12 sites, more work is needed to identify the optimal set of joints to be scanned in early gout. Finally, all these scanning protocols did not consider the patient's history [14,15,37,41]. Future studies should investigate the feasibility and accuracy of a flexible US scanning protocol that considers the sites most involved in the patient's history.

## 7. Sonographic Diagnosis of Gout in Undiagnosed Mono- or Oligoarthritis

The EULAR gout task force strongly recommends performing synovial fluid analysis in any patient with undiagnosed arthritis [8]. However, synovial fluid aspiration may not always be successful, and its analysis may lead to inconclusive results. In such conditions,

the US can provide an additional value over clinical data in the differential diagnosis of acute gout in patients presenting with acute arthritis [36,39,40].

In 2015, Zufferey et al. [39] carried out a monocentric and prospective study on 109 patients presenting with acute arthritis (including both gout and CPPD). The OMERACT US findings, indicative of MSU deposits, showed excellent specificity (92%) in the diagnosis of gout and moderate sensitivity (60%) when only the symptomatic joint was assessed. An increase in sensitivity (84%) and a concomitant decrease in specificity (78%) were observed when the scanning protocol considered other uninvolved joints, such as knees, ankles, and the MTP1 joints.

In 2017, similar results were observed by Pattamapaspong et al. [40]. In that study, the scanning protocol included only the clinically involved joint, in which synovial fluid analysis was performed (the knee in 64% of patients). The sensitivity and specificity of the OMERACT US findings indicative of MSU crystal deposits (DC sign and tophi) were 75% and 89%, respectively. Considering the US findings separately, the sensitivity and specificity were 42% and 92% for DC signs and 40% and 100% for tophi.

In 2023, Cipolletta et al. carried out a prospective study aimed at investigating the accuracy of US in the differential diagnosis between crystal arthritis (gout and CPPD) and other arthropathies in patients with acute mono/oligoarthritis [36]. Unlike previous studies, we adopted a flexible scanning protocol that considered the knees (femoral trochlear hyaline cartilage, menisci, patellar tendon, and popliteal groove region), the MTP1 joints, and the symptomatic one(s) in the suspicion of gout. The sensitivity and specificity of the US were 75.0% and 91.0% when assessing the symptomatic joint(s) only, whereas they were 91% and 91% when using the whole scanning protocol ( $p < 0.05$ ).

## 8. Sonographic Evaluation of MSU Burden in Patients Diagnosed with Gout for Prognosis and Treatment Monitoring

An increasing number of studies evaluated the role of the US in monitoring gouty patients receiving urate-lowering therapy (ULT) and showed the disappearance of the DC sign and a decrease in tophus size after achieving a SU  $< 6$  mg/dL [30,33,41–43].

The reduction in US MSU deposits was associated with the target SU level but not with disease duration or baseline SU [43]. In fact, a higher decrease in tophus size and in the number of joints showing DC signs was noted in patients reaching an SUA  $< 5$  mg/dL than in those with an SUA between 5 and 6 mg/dL [43].

Although even a more pronounced effect was noted in a longer follow-up, the minimal period of ULT required to observe a significant reduction in DC sign was 3 months [30,33,42,43]. Of note, Peiteado et al. documented the persistence of at least a joint showing a DC sign in 28.6% of patients after 24 months of ULT. Of interest, the therapeutic goal of SU  $< 6$  mg/dL was not reached by any of them [42].

According to the available evidence, cartilage deposits seem easier to clear than tophaceous deposits. Although small tophi may dissolve within a few months, bigger or more compact tophi may require a longer time to disappear. Thus, the disappearance of the DC sign may be considered the earliest US sign of ULT efficacy [30]. In fact, the presence of DC signs decreased from 92.9% to 44.4% after 12 months of ULT, while tophi showed only a little decrease (from 93.4% to 80.2%). In addition, articular tophi seem to dissolve easier than those at the tendon level [33,41,42]. This observation was supported by Christiansen et al., who documented statistically significant decreases in tophi at the MTP1 joint after a 6-month follow-up but not at tendon level (triceps, quadriceps, and patellar tendons) [33]. One of the reasons may be linked to a lower vascularisation of tendons and, consequently, to a lower crystal clearance [42].

Close monitoring of MSU deposits may guide early treatment changes. In fact, a contextual reduction in both SUA levels and US MSU deposits would lead to maintaining the same treatment. Conversely, the lack of US changes may be indicative of the need to optimise the ULT. Moreover, the baseline US burden of MSU crystal deposits has been associated with the risk of future flares [46–48]. Thus, reliable and feasible estimation of the

MSU burden should be considered an essential prerequisite for monitoring MSU crystal dissolution and deciding when to stop gout flare prophylaxis [49].

Since the measurement of whole-body MSU deposits is not feasible in daily practice, circumscribing such estimation to a predetermined set of joints or to a single and representative anatomic area may be a feasible alternative approach.

It should be considered that the higher the number of scanned sites, the more precise the estimation of MSU burden at the patient level, but the longer it takes to examine them.

Only two scanning protocols have been used to monitor ULT efficacy so far. Peiteado et al. and Ebstein et al. performed a 4-joint evaluation (MTP1 joints and knees) for DC sign and tophi [42,43]. On the other hand, Christiansen et al. suggested including six joints [MTP1 joint (for tophi and DC), MTP2 joint, and knee (for DC)] and four tendons [peroneal tendons and distal portion of patellar tendon (for tophi)] [41]. However, to date, no comparative studies are available, and the optimal number of joints to be monitored in patients starting ULT is far from being defined.

Another strategy to evaluate the efficacy of ULT was the US-size monitoring of a single tophus [30,42,43]. In fact, the identification and monitoring of only one index tophus, instead of many of them, would make follow-up evaluations easier and more feasible. Several US methods of tophus measurement were described. In 2007, Perez-Ruiz et al. [50] attempted to measure both tophus volume and its maximal diameter in a prospective US study, reporting the smallest detectable difference of 1.27 mm<sup>3</sup> for volume and of 5.5 mm (23.0% of the average measures) for maximal diameter. On the other hand, in 2019, Ebstein et al. [43] evaluated the largest diameter of the tophus, considering a significant difference greater than 20% of the baseline measure. Both methods showed sensitivity to change during ULT, and a significant decrease in tophus size was observed only after 6 months [30,43]. However, the criteria to select the “ideal” index tophus were not perfectly defined, and all these factors (dimensions: large vs. small tophi; echostructure: dense and compact vs. soft and heterogeneous tophi; site: subcutaneous, tendinous, intra-articular) should be kept in mind when selecting an index tophus to be monitored.

Moreover, tophi are complex structures containing collections of MSU crystals surrounded by inflammatory cells and connective tissue. In a cross-sectional study, Pascart et al. showed that US and DECT provided different results in measuring tophi, with DECT generally yielding smaller volumes than US [51]. This could be explained by the fact that the US and DECT may evaluate different structural components of the tophus, and the US may poorly distinguish between urate and non-urate components [52]. Of note, Peiteado et al. documented that nearly 80% of patients still had one or more tophaceous deposits after 24 months of ULT, even when patients who reached and maintained SU < 6 mg/dL were considered [42]. This finding may be explained by the following hypotheses: first, a lower target of SU may be necessary for patients with US evidence of tophi similar to what is recommended by the EULAR for tophaceous gout; second, non-urate fibrous components of the tophi may still be detectable by the US even after a successful ULT.

Aggregates were the US finding with less tendency to decrease during the ULT [30,33,41]. The temporal evolution of MSU aggregates cannot be easily predictable; while some may disappear during ULT, others may originate from the dissolution of large tophi. Thus, although this finding has been shown to be sensitive to change during effective treatment, the role of aggregates in the monitoring of ULT is yet to be clarified.

Even though the US showed great potential in the identification and monitoring of MSU burdens, further studies should address some unresolved issues. Which is the best method to monitor the changes in MSU deposits (dichotomous, semiquantitative, or quantitative)? Which OMERACT US elementary lesions should be considered (cartilage deposits, tophi, or both)? Which is the best scanning protocol to monitor ULT (single joint vs. set of joints)? What is the definition of an index tophus, and how should it be measured?

## 9. Conclusions

The evolving landscape of US applications in the diagnosis and management of gout has witnessed significant advancements over the past decade. As highlighted in this narrative review, the US has emerged as a valuable tool for detecting MSU crystal deposits, assessing disease burden, and monitoring treatment efficacy. For all these applications, the optimisation of the scanning technique plays a pivotal role in maximising the diagnostic potential of US in gout.

While for some gout clinical settings, a quite definite scanning protocol can be indicated, others still need to be further investigated.

Of note, the application of the US to the prognosis and treatment monitoring of gout reveals intriguing possibilities. The correlation between MSU burden and the risk of future flares underscores the potential of the US as a prognostic tool. Yet, the determination of the most effective and feasible set of joints for monitoring, especially in the early stages of gout or during urate-lowering therapy, requires further exploration.

While the US has demonstrated its utility in monitoring urate-lowering therapy and providing insights into the dynamic changes in MSU deposits, several questions persist. The optimal method for monitoring changes in MSU deposits, the choice between dichotomous, semiquantitative, or quantitative assessments, and the definition of an index tophus necessitate dedicated research efforts.

As more and more rheumatologists incorporate the US into their daily practice, the integration of evolving evidence with individual clinical experience will guide the optimal use of this imaging modality. The journey toward harnessing the full potential of the US in gout is ongoing, promising, and exciting.

**Author Contributions:** Conceptualization, E.C., E.F., G.F. and S.S. writing—original draft preparation, E.C.; writing—review and editing, E.F., G.F. and S.S.; supervision, E.F. and G.F. All authors have read and agreed to the published version of the manuscript.

**Funding:** The article publishing charge was funded by the Gout, Hyperuricemia and Crystal-Associated Disease Network (G-CAN).

**Institutional Review Board Statement:** Not applicable.

**Informed Consent Statement:** Not applicable.

**Data Availability Statement:** All the data are included in the manuscript and its references.

**Conflicts of Interest:** The authors declare no conflicts of interest.

## References

1. Dalbeth, N.; Merriman, T.R.; Stamp, L.K. Gout. *Lancet* **2016**, *388*, 2039–2052. [[CrossRef](#)] [[PubMed](#)]
2. Dehlin, M.; Jacobsson, L.; Roddy, E. Global epidemiology of gout: Prevalence, incidence, treatment patterns and risk factors. *Nat. Rev. Rheumatol.* **2020**, *16*, 380–390. [[CrossRef](#)] [[PubMed](#)]
3. Zhu, Y.; Pandya, B.J.; Choi, H.K. Prevalence of gout and hyperuricemia in the US general population: The National Health and Nutrition Examination Survey 2007–2008. *Arthritis Rheum.* **2011**, *63*, 3136–3141. [[CrossRef](#)]
4. Singh, J.A.; Gaffo, A. Gout epidemiology and comorbidities. *Semin. Arthritis Rheum.* **2020**, *50*, S11–S16. [[CrossRef](#)]
5. Cipolletta, E.; Tata, L.J.; Nakafero, G.; Avery, A.J.; Mamas, M.A.; Abhishek, A. Association Between Gout Flare and Subsequent Cardiovascular Events Among Patients with Gout. *JAMA* **2022**, *328*, 440–450. [[CrossRef](#)]
6. Clarson, L.; Chandratne, P.; Hider, S.; Belcher, J.; Heneghan, C.; Roddy, E.; Mallen, C. Increased cardiovascular mortality associated with gout: A systematic review and meta-analysis. *Eur. J. Prev. Cardiol.* **2015**, *22*, 335–343. [[CrossRef](#)]
7. Neogi, T.; Jansen, T.L.T.A.; Dalbeth, N.; Fransen, J.; Schumacher, H.R.; Berendsen, D.; Brown, M.; Choi, H.; Edwards, N.L.; Janssens, H.J.E.M.; et al. 2015 Gout Classification Criteria: An American College of Rheumatology/European League Against Rheumatism collaborative initiative. *Arthritis Rheumatol.* **2015**, *67*, 2557–2568. [[CrossRef](#)] [[PubMed](#)]
8. Richette, P.; Doherty, M.; Pascual, E.; Barskova, V.; Becce, F.; Castaneda, J.; Coyfish, M.; Guillo, S.; Jansen, T.; Janssens, H.; et al. 2018 updated European League Against Rheumatism evidence-based recommendations for the diagnosis of gout. *Ann. Rheum. Dis.* **2020**, *79*, 31–38. [[CrossRef](#)]
9. Dalbeth, N.; Doyle, A.J. Imaging of gout: An overview. *Best. Pract. Res. Clin. Rheumatol.* **2012**, *26*, 823–838. [[CrossRef](#)]

10. Ogdie, A.; Taylor, W.J.; Neogi, T.; Fransen, J.; Jansen, T.L.; Schumacher, H.R.; Louthrenoo, W.; Vazquez-Mellado, J.; Eliseev, M.; McCarthy, G.; et al. Performance of Ultrasound in the Diagnosis of Gout in a Multicenter Study: Comparison with Monosodium Urate Monohydrate Crystal Analysis as the Gold Standard. *Arthritis Rheumatol.* **2017**, *69*, 429–438. [[CrossRef](#)]
11. Grassi, W.; Okano, T.; Filippucci, E. Use of ultrasound for diagnosis and monitoring of outcomes in crystal arthropathies. *Curr. Opin. Rheumatol.* **2015**, *27*, 147–155. [[CrossRef](#)] [[PubMed](#)]
12. Filippucci, E.; Reginato, A.M.; Thiele, R.G. Imaging of crystalline arthropathy in 2020. *Best Pract. Res. Clin. Rheumatol.* **2020**, *34*, 101595. [[CrossRef](#)] [[PubMed](#)]
13. Christiansen, S.N.; Østergaard, M.; Terslev, L. Ultrasonography in gout: Utility in diagnosis and monitoring. *Clin. Exp. Rheumatol.* **2018**, *36* (Suppl. S114), 61–67. [[PubMed](#)]
14. Peiteado, D.; De Miguel, E.; Villalba, A.; Ordóñez, M.C.; Castillo, C.; Martín-Mola, E. Value of a short four-joint ultrasound test for gout diagnosis: A pilot study. *Clin. Exp. Rheumatol.* **2012**, *30*, 830–837. [[PubMed](#)]
15. Naredo, E.; Uson, J.; Jiménez-Palop, M.; Martínez, A.; Vicente, E.; Brito, E.; Rodríguez, A.; Cornejo, F.J.; Castañeda, S.; Martínez, M.J.; et al. Ultrasound-detected musculoskeletal urate crystal deposition: Which joints and what findings should be assessed for diagnosing gout? *Ann. Rheum. Dis.* **2014**, *73*, 1522–1528. [[CrossRef](#)] [[PubMed](#)]
16. Terslev, L.; Gutierrez, M.; Christensen, R.; Balint, P.V.; Bruyn, G.A.; Sedie, A.D.; Filippucci, E.; Garrido, J.; Hammer, H.B.; Iagnocco, A.; et al. Assessing Elementary Lesions in Gout by Ultrasound: Results of an OMERACT Patient-based Agreement and Reliability Exercise. *J. Rheumatol.* **2015**, *42*, 2149–2154. [[CrossRef](#)] [[PubMed](#)]
17. Cazenave, T.; Pan-American League of Associations for Rheumatology (PANLAR) Ultrasound Study Group; Martire, V.; Reginato, A.M.; Gutierrez, M.; Waimann, C.A.; Pineda, C.; Rosa, J.E.; Ruta, S.; Sedano-Santiago, O.; et al. Reliability of OMERACT ultrasound elementary lesions in gout: Results from a multicenter exercise. *Rheumatol. Int.* **2019**, *39*, 707–713. [[CrossRef](#)] [[PubMed](#)]
18. Christiansen, S.N.; Filippou, G.; Scirè, C.A.; Balint, P.V.; Bruyn, G.A.; Dalbeth, N.; DeJaco, C.; Sedie, A.D.; Filippucci, E.; Hammer, H.B.; et al. Consensus-based semi-quantitative ultrasound scoring system for gout lesions: Results of an OMERACT Delphi process and web-reliability exercise. *Semin. Arthritis Rheum.* **2021**, *51*, 644–649. [[CrossRef](#)]
19. Filippou, G.; Sirotti, S.; Cipolletta, E.; Filippucci, E. Optimising the use of ultrasound in CPPD: A review from the ground up. *Gout Urate Cryst. Depos. Dis.* **2024**, *2*, 17–33. [[CrossRef](#)]
20. Filippou, G.; Pacini, G.; Sirotti, S.; Zadory, M.; Carboni, D.; Damiani, A.; Fiorentini, E.; Cipolletta, E.; Filippucci, E.; Froehlich, J.M.; et al. Comparison of ultrasound attenuation by calcium pyrophosphate, hydroxyapatite and monosodium urate crystals: A proof-of-concept study. *Ann. Rheum. Dis.* **2022**, *81*, 1199–1201. [[CrossRef](#)]
21. Filippucci, E.; Di Geso, L.; Grassi, W. Tips and tricks to recognize microcrystalline arthritis. *Rheumatology* **2012**, *51* (Suppl. S7), vii18–vii21. [[CrossRef](#)] [[PubMed](#)]
22. Lee, Y.H.; Song, G.G. Diagnostic accuracy of ultrasound in patients with gout: A meta-analysis. *Semin. Arthritis Rheum.* **2018**, *47*, 703–709. [[CrossRef](#)]
23. Cipolletta, E.; Di Matteo, A.; Smerilli, G.; Di Carlo, M.; Di Battista, J.; Abhishek, A.; Grassi, W.; Filippucci, E. Ultrasound findings of calcium pyrophosphate deposition disease at metacarpophalangeal joints. *Rheumatology* **2022**, *61*, 3997–4005. [[CrossRef](#)] [[PubMed](#)]
24. Löffler, C.; Sattler, H.; Peters, L.; Löffler, U.; Uppenkamp, M.; Bergner, R. Distinguishing gouty arthritis from calcium pyrophosphate disease and other arthritides. *J. Rheumatol.* **2015**, *42*, 513–520. [[CrossRef](#)]
25. Löffler, C.; Sattler, H.; Löffler, U.; Krämer, B.K.; Bergner, R. Size matters: Observations regarding the sonographic double contour sign in different joint sizes in acute gouty arthritis. Die Größe macht den Unterschied: Beobachtungen zum sonographischen Doppelkonturzeichen in unterschiedlichen Gelenken bei akuter Gichtarthritis. *Z. Rheumatol.* **2018**, *77*, 815–823. [[CrossRef](#)] [[PubMed](#)]
26. Filippucci, E.; Riveros, M.G.; Georgescu, D.; Salaffi, F.; Grassi, W. Hyaline cartilage involvement in patients with gout and calcium pyrophosphate deposition disease. *An. Ultrasound Study Osteoarthr. Cartil.* **2009**, *17*, 178–181. [[CrossRef](#)]
27. Cipolletta, E.; Abhishek, A.; Di Matteo, A.; Grassi, W.; Filippucci, E. Dynamic assessment of the double contour sign by ultrasonography helps to distinguish between gout and calcium pyrophosphate deposition disease. *RMD Open* **2023**, *9*, e002940. [[CrossRef](#)]
28. Christiansen, S.N.; Østergaard, M.; Slot, O.; Fana, V.; Terslev, L. Ultrasound for the diagnosis of gout—the value of gout lesions as defined by the Outcome Measures in Rheumatology ultrasound group. *Rheumatology* **2021**, *60*, 239–249. [[CrossRef](#)] [[PubMed](#)]
29. Wright, S.A.; Filippucci, E.; McVeigh, C.; Grey, A.; McCarron, M.; Grassi, W.; Wright, G.D.; Taggart, A.J. High-resolution ultrasonography of the first metatarsal phalangeal joint in gout: A controlled study. *Ann. Rheum. Dis.* **2007**, *66*, 859–864. [[CrossRef](#)]
30. Hammer, H.B.; Karoliussen, L.; Terslev, L.; Haavardsholm, E.A.; Kvien, T.K.; Uhlig, T. Ultrasound shows rapid reduction of crystal depositions during a treat-to-target approach in gout patients: 12-month results from the NOR-Gout study. *Ann. Rheum. Dis.* **2020**, *79*, 1500–1505. [[CrossRef](#)]
31. Zayat, A.S.; Ellegaard, K.; Conaghan, P.G.; Terslev, L.; Hensor, E.M.A.; Freeston, J.E.; Emery, P.; Wakefield, R.J. The specificity of ultrasound-detected bone erosions for rheumatoid arthritis. *Ann. Rheum. Dis.* **2015**, *74*, 897–903. [[CrossRef](#)]

32. Cipolletta, E.; Smerilli, G.; Di Matteo, A.; Di Battista, J.; Di Carlo, M.; Grassi, W.; Filippucci, E. The sonographic identification of cortical bone interruptions in rheumatoid arthritis: A morphological approach. *Ther. Adv. Musculoskelet. Dis.* **2021**, *13*, 1759720X211004326. [[CrossRef](#)]
33. Christiansen, S.N.; Østergaard, M.; Slot, O.; Keen, H.; Bruyn, G.A.W.; D'Agostino, M.A.; Terslev, L. Assessing the sensitivity to change of the OMERACT ultrasound structural gout lesions during urate-lowering therapy. *RMD Open* **2020**, *6*, e001144. [[CrossRef](#)] [[PubMed](#)]
34. Bursill, D.; Taylor, W.J.; Terkeltaub, R.; Abhishek, A.; So, A.K.; Vargas-Santos, A.B.; Gaffo, A.L.; Rosenthal, A.; Tausche, A.-K.; Reginato, A.; et al. Gout, Hyperuricaemia and Crystal-Associated Disease Network (G-CAN) consensus statement regarding labels and definitions of disease states of gout. *Ann. Rheum. Dis.* **2019**, *78*, 1592–1600. [[CrossRef](#)]
35. Abhishek, A.; Courtney, P.; Jenkins, W.; Sandoval-Plata, G.; Jones, A.C.; Zhang, W.; Doherty, M. Brief Report: Monosodium Urate Monohydrate Crystal Deposits Are Common in Asymptomatic Sons of Patients with Gout: The Sons of Gout Study. *Arthritis Rheumatol.* **2018**, *70*, 1847–1852. [[CrossRef](#)]
36. Cipolletta, E.; Filippucci, E.; Abhishek, A.; Di Battista, J.; Smerilli, G.; Di Carlo, M.; Silveri, F.; De Angelis, R.; Salaffi, F.; Grassi, W.; et al. In patients with acute mono/oligoarthritis, a targeted ultrasound scanning protocol shows great accuracy for the diagnosis of gout and CPPD. *Rheumatology* **2023**, *62*, 1493–1500. [[CrossRef](#)]
37. Norkuviene, E.; Petraitis, M.; Apanaviciene, I.; Virviciute, D.; Baranauskaite, A. An optimal ultrasonographic diagnostic test for early gout: A prospective controlled study. *J. Int. Med. Res.* **2017**, *45*, 1417–1429. [[CrossRef](#)] [[PubMed](#)]
38. Lamers-Karnebeek, F.B.; Van Riel, P.L.; Jansen, T.L. Additive value for ultrasonographic signal in a screening algorithm for patients presenting with acute mono-/oligoarthritis in whom gout is suspected. *Clin. Rheumatol.* **2014**, *33*, 555–559. [[CrossRef](#)] [[PubMed](#)]
39. Zufferey, P.; Valcov, R.; Fabreguet, I.; Dumusc, A.; Omoumi, P.; So, A. A prospective evaluation of ultrasound as a diagnostic tool in acute microcrystalline arthritis. *Arthritis Res. Ther.* **2015**, *17*, 188. [[CrossRef](#)]
40. Pattamapaspong, N.; Vuthiwong, W.; Kanthawang, T.; Louthrenoo, W. Value of ultrasonography in the diagnosis of gout in patients presenting with acute arthritis. *Skeletal Radiol.* **2017**, *46*, 759–767. [[CrossRef](#)]
41. Christiansen, S.N.; Østergaard, M.; Slot, O.; Fana, V.; Terslev, L. Retrospective longitudinal assessment of ultrasound gout lesions using the OMERACT semi-quantitative scoring system. *Rheumatology* **2022**, *61*, 4711–4721. [[CrossRef](#)]
42. Peiteado, D.; Villalba, A.; Martín-Mola, E.; Balsa, A.; De Miguel, E. Ultrasound sensitivity to changes in gout: A longitudinal study after two years of treatment. *Clin. Exp. Rheumatol.* **2017**, *35*, 746–751. [[PubMed](#)]
43. Ebstein, E.; Forien, M.; Norkuviene, E.; Richette, P.; Mouterde, G.; Daien, C.; Ea, H.-K.; Brière, C.; Lioté, F.; Petraitis, M.; et al. Ultrasound evaluation in follow-up of urate-lowering therapy in gout: The USEFUL study. *Rheumatology* **2019**, *58*, 410–417. [[CrossRef](#)] [[PubMed](#)]
44. Bhadu, D.; Das, S.K.; Wakhlu, A.; Dhakad, U.; Sharma, M. Ultrasonographic detection of double contour sign and hyperechoic aggregates for diagnosis of gout: Two sites examination is as good as six sites examination. *Int. J. Rheum. Dis.* **2018**, *21*, 523–531. [[CrossRef](#)] [[PubMed](#)]
45. Zhang, B.; Yang, M.; Wang, H. Diagnostic value of ultrasound versus dual-energy computed tomography in patients with different stages of acute gouty arthritis. *Clin. Rheumatol.* **2020**, *39*, 1649–1653. [[CrossRef](#)] [[PubMed](#)]
46. Cipolletta, E.; Di Battista, J.; Di Carlo, M.; Di Matteo, A.; Salaffi, F.; Grassi, W.; Filippucci, E. Sonographic estimation of monosodium urate burden predicts the fulfillment of the 2016 remission criteria for gout: A 12-month study. *Arthritis Res. Ther.* **2021**, *23*, 185. [[CrossRef](#)] [[PubMed](#)]
47. Cipolletta, E.; Abhishek, A.; Di Battista, J.; Grassi, W.; Filippucci, E. Ultrasonography in the prediction of gout flares: A 12-month prospective observational study. *Rheumatology* **2023**, *62*, 1108–1116. [[CrossRef](#)]
48. Zou, Z.; Yang, M.; Wang, Y.; Zhang, B. Association of urate deposition shown by ultrasound and frequent gout attacks. Zusammenhang zwischen sonographisch darstellbarer Uratablagerung und häufigen Gichtanfällen. *Z. Rheumatol.* **2021**, *80*, 565–569. [[CrossRef](#)]
49. Ebstein, E.; Forien, M.; Norkuviene, E.; Richette, P.; Mouterde, G.; Daien, C.; Ea, H.-K.; Brière, C.; Lioté, F.; Petraitis, M.; et al. Ultrasound evaluation in follow-up of urate-lowering therapy in gout phase 2 (USEFUL-2): Duration of flare prophylaxis. *Jt. Bone Spine* **2020**, *87*, 647–651. [[CrossRef](#)]
50. Perez-Ruiz, F.; Martin, I.; Canteli, B. Ultrasonographic measurement of tophi as an outcome measure for chronic gout. *J. Rheumatol.* **2007**, *34*, 1888–1893.
51. Pascart, T.; Grandjean, A.; Norberciak, L.; Ducoulombier, V.; Motte, M.; Luraschi, H.; Vandecandelaere, M.; Godart, C.; Hovenagel, E.; Namane, N.; et al. Ultrasonography and dual-energy computed tomography provide different quantification of urate burden in gout: Results from a cross-sectional study. *Arthritis Res. Ther.* **2017**, *19*, 171. [[CrossRef](#)] [[PubMed](#)]
52. Modjinou, D.V.; Krasnokutsky, S.; Gyftopoulos, S.; Pike, V.C.; Karis, E.; Keenan, R.T.; Lee, K.; Crittenden, D.B.; Samuels, J.; Pillinger, M.H. Comparison of dual-energy CT, ultrasound and surface measurement for assessing tophus dissolution during rapid urate debulking. *Clin. Rheumatol.* **2017**, *36*, 2101–2107. [[CrossRef](#)] [[PubMed](#)]

**Disclaimer/Publisher's Note:** The statements, opinions and data contained in all publications are solely those of the individual author(s) and contributor(s) and not of MDPI and/or the editor(s). MDPI and/or the editor(s) disclaim responsibility for any injury to people or property resulting from any ideas, methods, instructions or products referred to in the content.